$\alpha_4\beta_1$-dependent adhesion strengthening under mechanical strain is regulated by paxillin association with the α_4-cytoplasmic domain

Ronen Alon,[1] Sara W. Feigelson,[1] Eugenia Manevich,[1] David M. Rose,[2] Julia Schmitz,[3] Darryl R. Overby,[4,5] Eitan Winter,[1] Valentin Grabovsky,[1] Vera Shinder,[1] Benjamin D. Matthews,[4,5,6] Maya Sokolovsky-Eisenberg,[1] Donald E. Ingber,[4,5] Martin Benoit,[3] and Mark H. Ginsberg[2]

[1]Department of Immunology, The Weizmann Institute of Science, Rehovot 76100, Israel
[2]Department of Medicine, University of California, San Diego, La Jolla, CA 9209
[3]Center for Nano Science, Ludwigs-Maximilians-Universität, Munich D-80799, Germany
[4]Department of Pathology and [5]Department of Surgery, Vascular Biology Program, Children's Hospital, and [6]Department of Pediatrics, Massachusetts General Hospital, Harvard Medical School, Boston, MA 02115

The capacity of integrins to mediate adhesiveness is modulated by their cytoplasmic associations. In this study, we describe a novel mechanism by which α_4-integrin adhesiveness is regulated by the cytoskeletal adaptor paxillin. A mutation of the α_4 tail that disrupts paxillin binding, α_4(Y991A), reduced talin association to the $\alpha_4\beta_1$ heterodimer, impaired integrin anchorage to the cytoskeleton, and suppressed $\alpha_4\beta_1$-dependent capture and adhesion strengthening of Jurkat T cells to VCAM-1 under shear stress. The mutant retained intrinsic avidity to soluble or bead-immobilized VCAM-1, supported normal cell spreading at short-lived contacts, had normal α_4-microvillar distribution, and responded to inside-out signals. This is the first demonstration that cytoskeletal anchorage of an integrin enhances the mechanical stability of its adhesive bonds under strain and, thereby, promotes its ability to mediate leukocyte adhesion under physiological shear stress conditions.

Introduction

Circulating leukocytes rapidly develop firm adhesion to vessel wall ligands through their various integrin receptors $\alpha_4\beta_7$, $\alpha_4\beta_1$ (VLA-4), $\alpha_L\beta_2$ (LFA-1), and $\alpha_M\beta_2$ (Mac-1; Alon and Feigelson, 2002). Integrins bind their respective endothelial ligands under shear flow at lower efficiency than selectins (Springer, 1994). Adhesive tethers form over a fraction of a second and depend on the ability of the nascent adhesive bond to withstand disruptive shear force. In contrast to selectins, all leukocyte integrins can undergo instantaneous up-regulation of their affinity or avidity to endothelial ligands upon exposure to endothelial chemokines (Kinashi, 2005). In addition, integrins can undergo conformational changes upon ligand binding (Hynes, 2002). Cytoskeletal constraints of integrins may also control integrin adhesiveness (van Kooyk and Figdor, 2000). Previous studies on leukocyte (L)-selectin function regulation have shown that preformed cytoskeletal associations of L-selectin with the actin cytoskeleton control the ability of ligand-occupied selectin to stabilize nascent tethers under shear flow and capture leukocytes under physiological shear stresses (Kansas et al., 1993; Dwir et al., 2001). This raised the possibility that specialized subsets capable of interacting with their respective endothelial ligands under physiological shear flow may also need to properly anchor to the cytoskeleton. Although selectins and integrins are structurally distinct, we hypothesized that α_4 integrin bonds forming under disruptive shear stresses may share a common regulatory mechanism with L-selectin bonds. However, as alterations in cytoskeletal constraints of integrins can modify affinity, clustering, and ligand-induced conformational rearrangements (Carman and Springer, 2003), the direct contribution of integrin anchorage to adhesive outcome has been difficult to dissect.

In this study, we unraveled novel adhesive properties of an α_4-tail mutant with disrupted association with the cytoskeletal adaptor paxillin (Liu et al., 1999). We found that blocking the α_4–paxillin interaction markedly impaired the integrin's ability to anchor to the cytoskeleton in Jurkat T cells. Although not essential for $\alpha_4\beta_1$ affinity, ligand-induced conformational

Correspondence to Ronen Alon: ronen.alon@weizmann.ac.il

D.R. Overby's present address is Department of Biomedical Engineering, Tulane University, New Orleans, LA 70118.

Abbreviations used in this paper: AFM, atomic force microscopy; HUVEC, human umbilical vein endothelial cell; siRNA, short inhibitory RNA; wt, wild type.

The online version of this article contains supplemental material.

The Journal of Cell Biology, Vol. 171, No. 6, December 19, 2005 1073–1084
http://www.jcb.org/cgi/doi/10.1083/jcb.200503155

Supplemental Material can be found at:
http://www.jcb.org/cgi/content/full/jcb.200503155/DC1

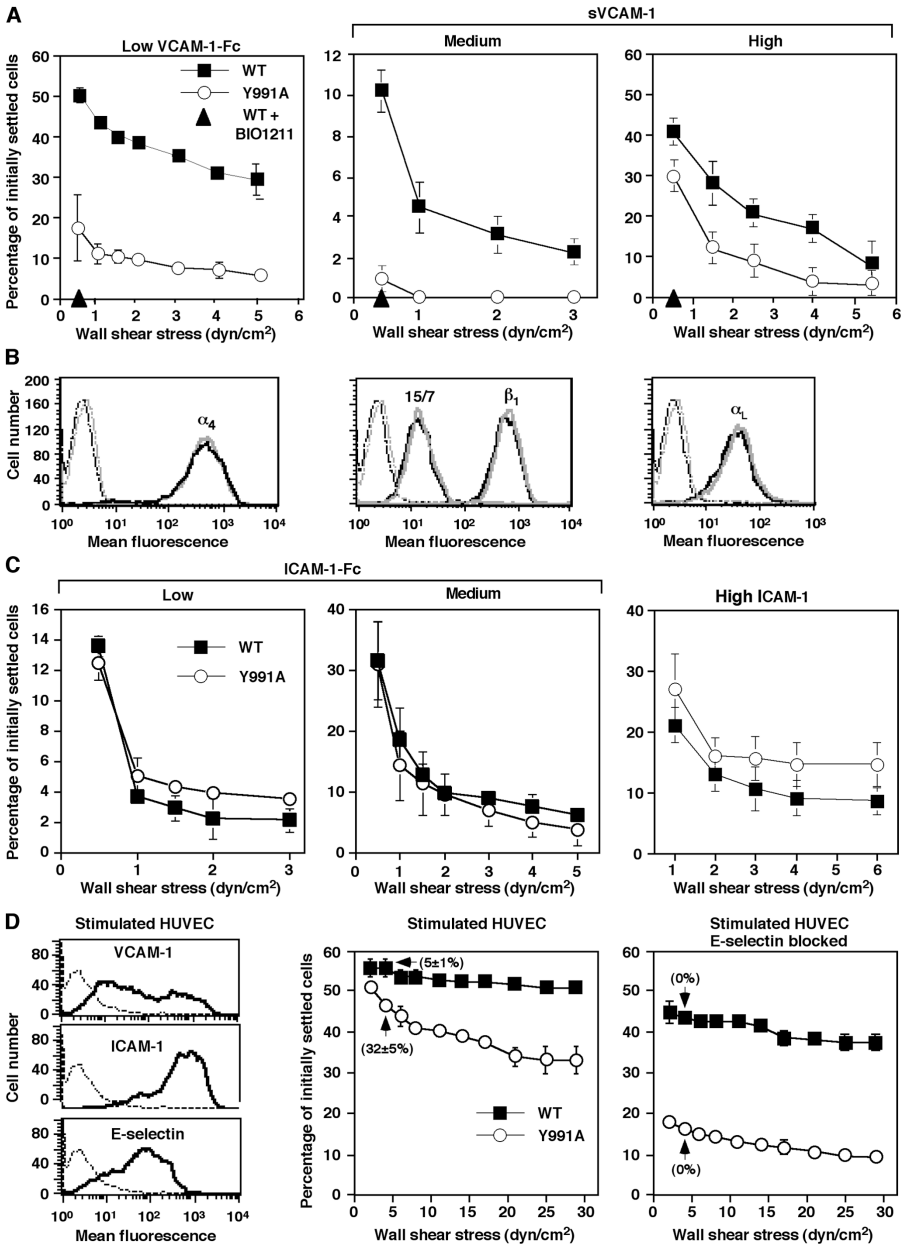

Figure 1. **The α_4(Y991A)β_1 mutant mediates poor shear-resistant adhesion to VCAM-1.** (A) JB4 Jurkat cells expressing either wt α_4 (WT) or the α_4(Y991A) mutant (Y991A) were settled for 1 min on low density VCAM-1–Fc (80 CAM sites/μm^2; left) or on sVCAM-1 coated at medium (1,480 sites/μm^2; middle) or high density (3,700 sites/μm^2; right), and their resistance to detachment by incremented shear stresses was analyzed. The fraction of cells within initially settled populations remaining bound at the end of each interval of shear increase is shown for each cell population. (B) FACS staining of ectopically expressed α_4, endogenous β_1 and α_L subunits, as well as of the β_1 activation neoepitope 15/7 on wt- and α_4(Y991A)-expressing JB4 cells, depicted with black and gray lines, respectively. (C) LFA-1–dependent adhesion of both wt- and α_4(Y991A)-expressing JB4 cells to low (80 sites/μm^2) or medium density ICAM-1–Fc (160 sites/μm^2) as well as to high density ICAM-1 (7,600 sites/μm^2), measured as in A. In each panel, the mean ± range of two experimental fields is depicted. Results in A and C are representative of six independent experiments. (D) FACS staining of VCAM-1, ICAM-1, and E-selectin on TNFα-stimulated HUVECs. Dotted lines represent staining of isotype-matched controls (left). VLA-4–dependent adhesion of JB4 cells transfected with wt α_4 (WT) or the α_4(Y991A) mutant to intact (left) or E-selectin–blocked TNFα-stimulated HUVECs (right). Resistance to the detachment of cells settled for 1 min on the monolayer was assessed as in A. Shown in parenthesis are the fractions of adherent cells that maintained rolling on the different HUVECs at 5 dyn/cm^2. LFA-1 blockage did not affect Jurkat resistance to detachment, whereas pretreatment with the $\alpha_4\beta_1$-specific blocker Bio1211 (at 1 μg/ml) resulted in complete loss of shear resistance (not depicted). Error bars represent SD.

changes, surface clustering and topography, or redistribution at short static contacts, paxillin association with $\alpha_4\beta_1$ was crucial for $\alpha_4\beta_1$–VCAM-1 bonds to resist mechanical stress. These results suggest that subsecond stabilization of α_4 tethers depends on the ability of ligand-occupied α_4 integrins to properly anchor to the cytoskeleton. This work also highlights the key role of the α subunit of $\alpha_4\beta_1$ in postligand binding adhesion strengthening of the integrin under mechanical strain.

Results

Paxillin association with the α_4-cytoplasmic domain is required for cell resistance to detachment by shear stress

Paxillin binding to the α_4-cytoplasmic domain is important for integrin $\alpha_4\beta_1$ signaling but not for adhesion developed in shear-free conditions (Rose et al., 2003). To examine the role of paxillin binding in $\alpha_4\beta_1$-mediated adhesion under shear stress, we analyzed the resistance to shear-induced detachment from the $\alpha_4\beta_1$ ligand VCAM-1 of α_4-deficient JB4 Jurkat T cells transfected with either wild-type (wt) α_4 (JB4-wt) or the paxillin binding–defective α_4(Y991A) mutant JB4-α_4(Y991A) (Rose et al., 2003). JB4-α_4(Y991A) cells were less resistant to shear-induced detachment than their JB4-wt counterparts (Fig. 1 A). Notably, bivalent VCAM-1 (VCAM-1–Fc) was much more potent than monovalent soluble VCAM-1 (sVCAM-1) in supporting $\alpha_4\beta_1$-specific adhesion (Fig. 1 A), but it still could not rescue the adhesive defect of the α_4(Y991A) mutant. These results were confirmed with multiple clones expressing similar levels of α_4 and β_1 subunits as well as the β_1 activation epitope 15/7 (Fig. 1 B and not depicted). Nevertheless, resistance to detachment from different densities of either ICAM-1–Fc or

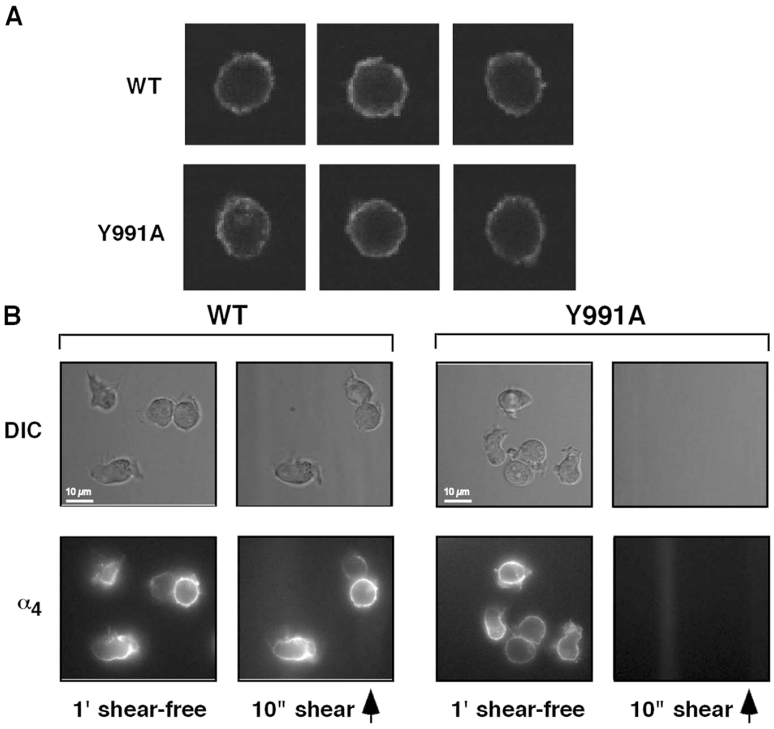

Figure 2. **The α_4(Y991A)β_1 mutant distributes normally before and during early cell spreading on VCAM-1 in shear-free conditions.** (A) wt α_4 or α_4(Y991A) is evenly distributed on the surface of JB4 cells. Confocal immunostaining of α_4 on the surface of prefixed WT or Y991A cells using the non-blocking B5G10 mAb. Three representative cells are shown for each cell type. (B) Live imaging of wt α_4 or α_4(Y991A) during short cellular contacts with VCAM-1. JB4 cells expressing wt or mutant α_4 were prelabeled with AlexaFluor488-conjugated B5G10 mAb and settled for 1 min on VCAM-1. wt or mutant α_4 were each imaged on cells that had spread on sVCAM-1 for 1 min (shear free) and were then subjected to 10 s of shear stress at 2 dyn/cm^2. Cell morphology was monitored in differential interface microscopy (DIC). The degree of patching was calculated by Image J analysis and was defined as having at least one region with a B5G10 staining mean intensity threefold higher than another region on the same cell. Note that shear stress on its own did not trigger wt α_4 redistribution. Shear direction is depicted by the arrow.

ICAM-1 was comparable between wt- and mutant $\alpha_4\beta_1$–expressing cells (Fig. 1 C). In agreement with these results, VLA-4–dependent adhesion to TNFα-stimulated human umbilical vein endothelial cells (HUVECs) was reduced in Jurkat cells expressing the α_4(Y991A) mutant (Fig. 1 D), in particular at shear stresses ≥5 dyn/cm^2, within the upper range of shear stresses prevailing in postcapillary venules where the majority of lymphocyte extravasation takes place (Firrell and Lipowsky, 1989). Whereas most cells expressing the wt α_4 firmly arrested on the stimulated HUVEC via their VLA-4, a significant fraction of α_4(Y991A) mutant–expressing cells failed to arrest and established endothelial (E)-selectin–dependent rolling on the HUVEC (Fig. 1 D). In the absence of functional E-selectin, the shear resistance of cells expressing the α_4(Y991A) mutant was much lower than the shear resistance of cells expressing wt α_4 (Fig. 1 D). Because the contribution of LFA-1 to Jurkat arrest was minimal, these data suggest that the Y991A α_4 mutant is deficient in establishing $\alpha_4\beta_1$-mediated shear resistance on endothelial cells expressing VCAM-1 as well as on substrates coated with isolated VCAM-1.

Notably, preformed clustering of wt and mutant α_4 subunits on JB4 cells was essentially identical (Fig. 2 A). Real time imaging of JB4 cells that adhered on VCAM-1 also showed identical cell spreading as well as the distribution of both mutant and wt α_4 during 1-min cellular contacts before shear application (WT: n = 44, 16% round, 54% polarized with uniform α_4, 30% polarized with patched α_4; Y911A: n = 27, 18% round, 52% polarized with uniform α_4, 30% polarized with patched α_4; Fig. 2 B). Notably, the strength of resistance to detachment developed by wt α_4 did not correlate with the degree of patching (Fig. 2 B) in contrast to reports on LFA-1–dependent systems (Constantin et al., 2000; Kim et al., 2004). Thus, a mutation of the α_4 tail defective in paxillin binding prevents $\alpha_4\beta_1$-mediated resistance to shear-induced cell detachment independent of cell spreading and α_4 patching on VCAM-1.

The α_4(Y991A) mutation blocks paxillin association with the α_4 tail selectively (Liu et al., 1999). As an alternative test of the role of the α_4–paxillin interaction, we exploited a recently identified small molecule inhibitor of this interaction. The compound, designated A7B7C7, blocks the α_4–paxillin interaction and interferes with $\alpha_4\beta_1$-dependent cell migration (Ambroise et al., 2002). This inhibitor, but not a control compound (A6B6C6), attenuated the shear resistance of wt $\alpha_4\beta_1$–mediated Jurkat cell adhesion to VCAM-1 (Fig. 3 A, left) but had no effect on the residual shear resistance developed by the JB4-α_4(Y991A) cells (Fig. 3 A, right). Adhesion mediated by the $\alpha_L\beta_2$–ICAM-1 interaction was also insensitive to the inhibitor (not depicted). Knocking down paxillin expression by up to 75% using transient short inhibitory RNA (siRNA) silencing (Fig. 3 B) resulted in reduced adhesiveness of wt $\alpha_4\beta_1$–mediated Jurkat cell adhesion to VCAM-1 (Fig. 3 C), with no inhibition of adhesiveness mediated by the α_4(Y991A) mutant (Fig. 3 C). Notably, LFA-1–dependent adhesion to ICAM-1 was also insensitive to identical paxillin silencing (not depicted). Thus, both genetic and pharmacological approaches indicate that the α_4–paxillin interaction increases the resistance of $\alpha_4\beta_1$–VCAM-1 contacts to detachment by disruptive shear stresses.

Paxillin association with the α_4 subunit promotes $\alpha_4\beta_1$ anchorage to the cytoskeleton

Paxillin binds a number of actin-binding proteins such as talin and vinculin (Brown and Turner, 2004) and does so at sites distinct from the α_4-binding site (Liu and Ginsberg,

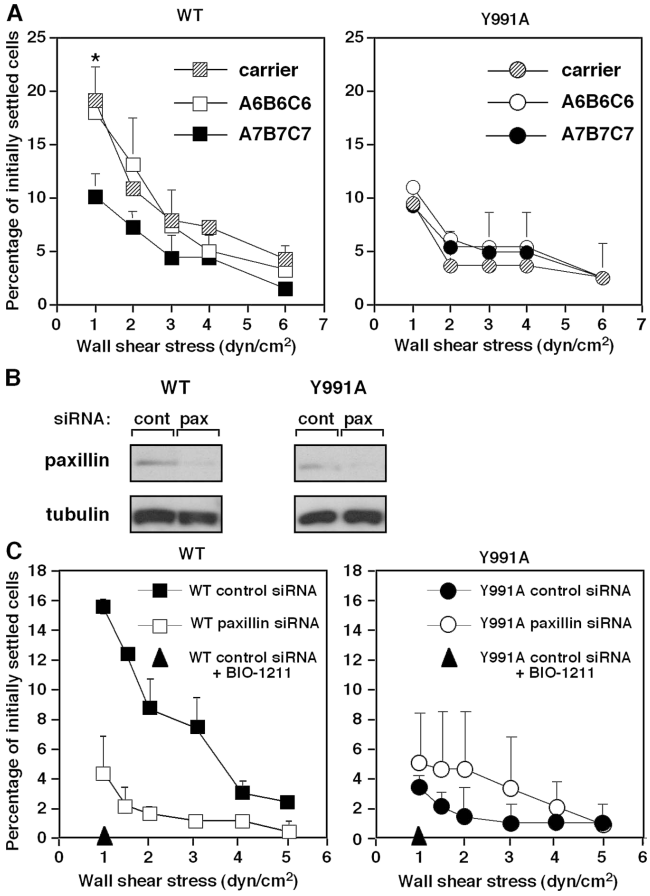

Figure 3. **Blockage of $\alpha_4\beta_1$ paxillin associations interferes with shear resistance developed by wt α_4.** (A) JB4 cells expressing either wt α_4 or α_4(Y991A) were pretreated for 15 min with A7B7C7, a cell-permeable inhibitor of paxillin binding to the α_4 tail, or with the control compound A6B6C6, both present at 5 μM. The shear resistance of carrier or compound-treated cells developed after 1-min adhesion to sVCAM-1 (2,220 sites/μm^2) was determined as in Fig. 1. Results are mean ± range of two experimental fields. The experiments depicted are each representative of four independent tests. *, $P < 0.001$ (a two-tailed paired *t* test) for control compared with A7B7C7-treated cells at 0.5 dyn/cm^2. (B) JB4 cells expressing wt α_4 were transfected with either paxillin-specific or control luciferase siRNA. Total lysates of each group were immunoblotted with paxillin- or tubulin-specific mAbs. Densitometric analysis reveals a decrease of 70 and 75% in paxillin content in JB4 expressing either wt or α_4(Y991A), respectively. (C) Paxillin silencing impairs resistance to detachment from sVCAM-1 developed by wt $\alpha_4\beta_1$ but not α_4(Y991A). The shear resistance of the indicated cells was determined as in A. Results are representative of three independent experiments. Error bars represent SD.

2000). We next quantified the fraction of detergent-resistant wt α_4 or α_4(Y991A) retained on NP-40–solubilized cells using fluorescence-tagged integrin-bound α_4 mAb (Fig. 4 A). Retention of intact wt and α_4(Y991A) was similar and low (20% of the total surface α_4; Fig. 4 A). However, the addition of anti–mouse Ig to cluster the mAb-bound wt α_4 markedly increased the association of $\alpha_4\beta_1$ surface integrin with the detergent-insoluble cytoskeleton (Fig. 4 B). In contrast, the same treatment produced a negligible increase in the cytoskeletal association of α_4(Y991A)β_1 (Fig. 4 B). Thus, the α_4(Y991A) mutant fails to anchor properly to the actin cytoskeleton in Jurkat T cells.

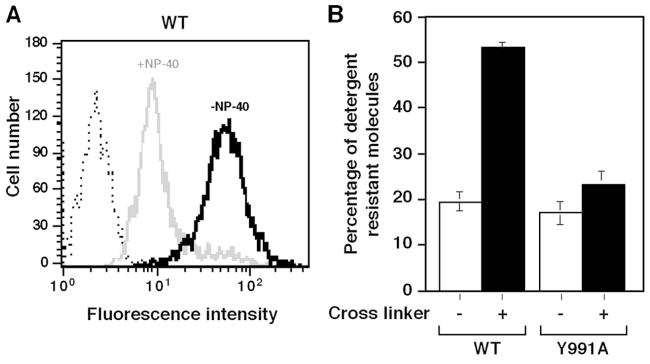

Figure 4. **Paxillin association with α_4 facilitates integrin anchorage to the cytoskeletal matrix.** (A) Detergent removal of nonligated wt α_4 monitored by FACS. Jurkat cells were reacted for 30 min at 4°C with FITC-conjugated anti-$\alpha_4\beta_1$ mAb (HP1/2) or isotype-matched control (dotted line). Cells were then incubated at RT in detergent-free buffer (black, −NP-40) or in buffer containing 0.05% NP-40 (gray, +NP-40). The fraction of α_4-bound mAb remaining after detergent treatment assessed by flow cytometry is shown relative to originally bound α_4 mAb. (B) The fraction of mAb-bound wt or α_4(Y991A) resistant to detergent-induced removal was compared before (white bars) and after ligation of the mAb by secondary antibody (black bars). Results are a mean of three independent experiments. Error bars represent SD.

The α_4(Y991A) mutant poorly associates with talin and does not respond to talin suppression

In light of this poor cytoskeletal anchorage of α_4(Y991A)β_1, we next compared the level of talin associated with the wt or mutant $\alpha_4\beta_1$ complex in nonadherent Jurkat cells. Notably, constitutive talin binding to the α_4(Y991A)β_1 complex was significantly reduced compared with the wt integrin, as was evident from coprecipitation analysis (Fig. 5 A). Knocking down up to 65% of the total talin content in wt $\alpha_4\beta_1$–expressing Jurkat cells (Fig. 5 B) retained integrin expression (not depicted) but resulted in significant reduction in their $\alpha_4\beta_1$-mediated shear resistance on both sVCAM-1 and VCAM-1–Fc (Fig. 5 C, left and right insets, respectively). Notably, identical suppression of talin expression in the α_4(Y991A)β_1-expressing Jurkat cells (Fig. 5 B) had no effect on their low shear resistant adhesion to identical VCAM-1 substrates (Fig. 5 C, right). These results collectively suggest that paxillin association with $\alpha_4\beta_1$ also recruits talin to the α_4–paxillin complex and may enhance talin association with the β_1 subunit tail. Thus, both paxillin and talin associations promote $\alpha_4\beta_1$-dependent cell resistance to detachment from VCAM-1 under shear stress.

α_4-Paxillin association is not required for $\alpha_4\beta_1$ avidity for VCAM-1 but increases α_4 bond stiffness

Although the affinity of integrin α_4(Y991A)β_1 to soluble VCAM-1–Fc is retained (Rose et al., 2003), we considered that Jurkat cells expressing the α_4(Y991A)β_1 mutant might fail to develop shear resistant adhesion as a result of reduced avidity for surface-bound VCAM-1. Comparing wt $\alpha_4\beta_1$ with α_4(Y991A)β_1 adhesiveness to VCAM-1–coated beads in the absence of applied shear stress, we found that JB4-wt and JB4-

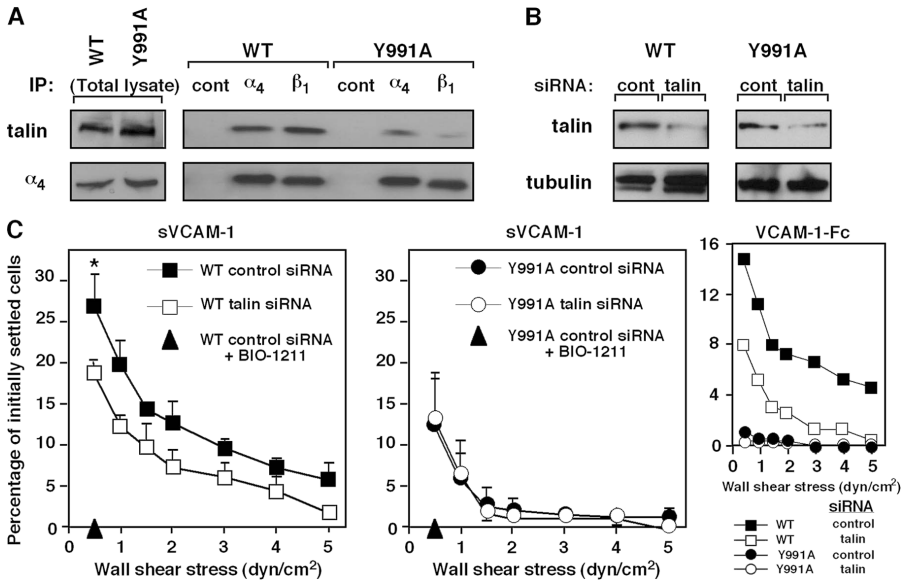

Figure 5. **The α_4(Y991A)β_1 mutant poorly associates with talin.** (A) The α_4(Y991A)β_1 complex does not properly recruit talin. Total lysates (left) or talin coprecipitating with anti-α_4, anti-β_1, or an irrelevant mouse IgG (right) from lysates of either JB4 transfected with wt α_4 or the α_4(Y991A) mutant (top). The blot was stripped and reprobed for α_4 (bottom). (B) Silencing of talin in JB4 cells expressing either wt or α_4(Y991A). The indicated cells were transfected with either talin1-specific or control siRNA. Total lysates of each group were immunoblotted with talin or tubulin-specific mAbs. Densitometric analysis reveals a decrease of 66 and 67% in talin content in JB4 expressing either wt or α_4(Y991A), respectively. (C) Talin suppression preferentially impairs wt $\alpha_4\beta_1$–mediated resistance to detachment from sVCAM-1 (2,220 sites/μm^2). *, $P < 0.03$ for control compared with talin-silenced cells at 0.5 dyn/cm^2. Where indicated, cells were pretreated with the $\alpha_4\beta_1$-specific blocker BIO1211. (inset) Effect of talin suppression on resistance to detachment from VCAM-1–Fc (30 CAM sites/μm^2) of JB4 cells expressing either wt or α_4(Y991A). In each panel, the mean ± range of two experimental fields is depicted. Results are representative of three independent experiments. Error bars represent SD.

α_4(Y991A) cells bound identically to magnetic beads coated with increasing site densities of VCAM-1–Fc (Fig. 6 A), which is supportive of the normal adhesion of α_4(Y991A)β_1-expressing cells under static conditions. Nevertheless, when VCAM-1–coated beads that bound to JB4-wt cells were exposed to abrupt mechanical stress, these beads were displaced significantly less than beads prebound to JB4-α_4(Y991A) cells (Fig. 6 B and Fig. S1, available at http://www.jcb.org/cgi/content/full/jcb.200503155/DC1). α_4 resistance to displacement required an intact actin cytoskeleton, as JB4-wt cells pretreated with the F-actin–severing drug cytochalasin D exhibited even greater displacement in response to abrupt magnetic stress (Fig. 6 C). These findings, together with the shear-based detachment assays (Fig. 1), collectively suggest that paxillin association with the $\alpha_4\beta1$ heterodimer and an intact actin cytoskeleton are both required for ligand-occupied $\alpha_4\beta_1$ to develop stress-resistant adhesive bonds.

Paxillin association with the α_4 tail augments α_4-mediated T cell capture on VCAM-1 and MadCAM-1 under shear flow

The $\alpha_4\beta_1$ and $\alpha_4\beta_7$ integrins mediate leukocyte capture under physiological shear flow (Alon et al., 1995; Berlin et al., 1995). Therefore, we compared the ability of mutant α_4(Y991A) versus wt α_4 to support $\alpha_4\beta_1$-dependent T cell capture by monovalent and bivalent VCAM-1 under continuous shear flow. Consistent with its defective resistance to shear force, α_4(Y991A)β_1 mediated reduced cell capture and arrest on a large range of densities of either monovalent (sVCAM) or bivalent (VCAM-Fc) VCAM-1 (Fig. 7, A and B). This differential behavior was also manifested at different levels of shear stress that were tested (Fig. 7 B, first two panels). Notably, whereas disruption of the actin cytoskeleton by cytochalasin D resulted in marked inhibition of both cell capture and arrest mediated by wt $\alpha_4\beta_1$, cytochalasin D had no effect on the residual adhesions mediated by the α_4(Y991A)β_1 mutant (Fig. 7 A). Interestingly, the duration of individual $\alpha_4\beta_1$ tethers, which is a measure of integrin affinity to the ligand (Feigelson et al., 2001), was not altered upon the loss of paxillin binding (Fig. 7 A). Thus, for optimal cell capture under shear flow, the α_4 tail of $\alpha_4\beta_1$ requires associations with the intact actin cytoskeleton.

Jurkat cells express low levels of the β_7 integrin subunit; thus, >95% of their α_4-integrin subunits are found in $\alpha_4\beta_1$ heterodimers. Nevertheless, JB4-wt cell capture on high density of the bivalent $\alpha_4\beta_7$-integrin ligand MadCAM-1–Fc (Berlin et al., 1993) was inhibited by the anti-$\alpha_4\beta_7$ antibody Act-1 (unpublished data). The JB4-α_4(Y991A) cells formed fivefold fewer tethers on MadCAM-1 than JB4-wt cells, with a diminished fraction of tethers followed by immediate arrests (Fig. 7 B, right). Thus, paxillin association with the α_4 subunit enhances the ability of α_4 to promote adhesive tethers in the context of both β_1 and β_7 integrins under continuously applied disruptive shear stress.

Preferential localization of receptors to microvilli increases their availability for interactions with counter ligands under shear flow (von Andrian et al., 1995). Electron microscopic analysis of wt α_4 and the α_4(Y991A)-tail mutant revealed identical distribution of these variants to microvillar compartments (82 ± 4% for wt α_4, $n = 222$; 80 ± 6% for the α_4(Y991A) mutant, $n = 196$; Fig. 5 C). Furthermore, a higher ratio of the α_4(Y991A)-tail mutant localized on microvillar tips than wt α_4 (a 4.5 tip/base ratio for the mutant vs. only 1.8 tip/base ratio for wt α_4). The number and size of microvillar projections in JB4-wt and JB4-α_4(Y991A) cells were also comparable (Fig. 7 C). Thus, the enhanced ability of wt $\alpha_4\beta_1$ to

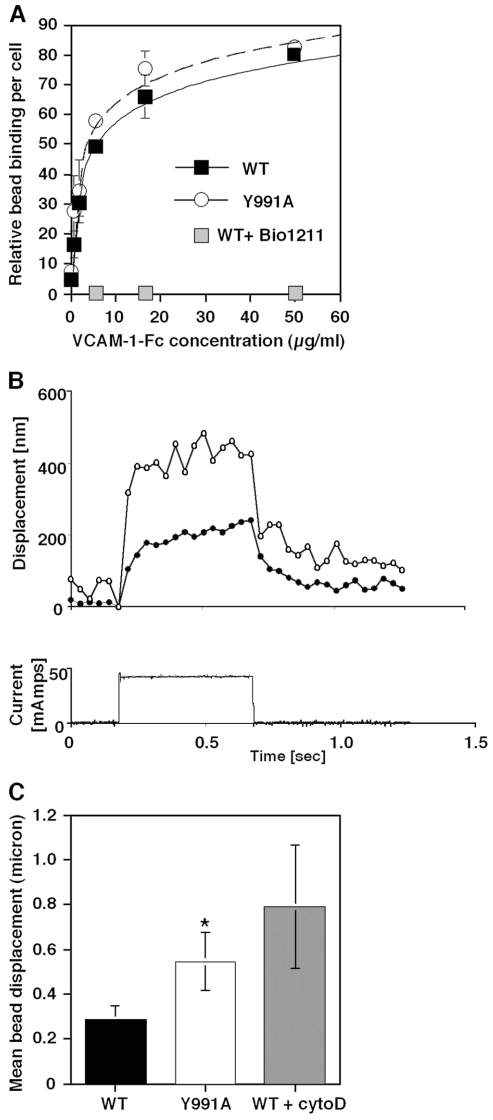

Figure 6. **The α_4(Y991A)β_1 mutant exhibits normal avidity under shear-free conditions but develops lower bond stiffness under applied force.** (A) Binding of either wt or Y991A $\alpha_4\beta_1$-expressing cells to M-280 protein A Dynabeads coated with 2D VCAM-1–Fc. Relative bead binding was determined by side scattering analysis. Bead binding in the presence of 1 μg/ml of the $\alpha_4\beta_1$-specific blocker Bio1211 is shown in gray squares. Results are representative of three independent experiments. (B, top) Representative bead displacement measured from an α_4(Y991A)-expressing cell (open circles) and a wt α_4–expressing cell (closed circles) during a 500-ms force pulse of ~100 pN. (bottom) Electromagnetic current waveform corresponding to the displacement response. (C) VCAM-1–coated magnetic bead displacement in response to magnetic force pulse. VCAM-1 beads bound on the surface of JB4 cells expressing wt or α_4(Y991A) as well as on cytochalasin D–treated JB4 cells expressing wt α_4 were exposed for 0.5 s to the force pulse as described in the supplemental Materials and methods and Fig. S1 (available at http://www.jcb.org/cgi/content/full/jcb.200503155/DC1). For each experimental group, 8–10 cells were analyzed, and results are the mean ± SD (error bars) of all displacement curves. All samples were confirmed by side scattering analysis to bind a similar number of VCAM-1 beads. A two-tailed unpaired *t* test for mean bead displacements on wt and α_4(Y991A)-expressing JB4 cells yielded $P < 0.06$. One representative experiment of three.

promote adhesive tethers under shear flow was not the result of its preferential distribution to cellular microvilli or to increased localization on microvillar tips.

The α_4(Y991A)β_1 mutant fails to generate productive adhesive bonds with VCAM-1 under disruptive forces

To examine the effects of disrupting the α_4–paxillin interaction at a single molecule level and in the presence of an external force other than shear stress, we next measured the force of unitary adhesive interactions between wt $\alpha_4\beta_1$ or the α_4(Y991A)β_1 mutant and immobilized VCAM-1 by atomic force microscopy (AFM). JB4-wt or JB4-α(Y991A) cells were coupled to the end of an AFM cantilever (Fig. 8 A) and lowered onto a VCAM-1–Fc-coated surface. After a 0.5-s contact, the frequency of productive adhesive events and their strength were analyzed by the degree of deflection experienced by the cantilever during its retraction from the adhesive substrate. Both cell types detached from the VCAM-1 substrate through single jumps, suggesting the breakage of individual bonds during cantilever retraction (Fig. 8 B). The adhesion frequencies of all experiments were maintained below 30%, a level assumed to reflect single $\alpha_4\beta_1$–VCAM-1 interactions (Zhang et al., 2004). The specificity of the adhesive events detected in this system were confirmed by a similar 70% reduction in total binding events by the blockade of wt $\alpha_4\beta_1$ with Bio1211 (Lin et al., 1999) or by omission of VCAM-1 from the substrate (Fig. 8 C and not depicted). As indicated by the force histograms derived for JB4-wt or JB4-α_4(Y991A) cells (Fig. 8 C), the frequency of productive adhesive events developed by α_4(Y991A)β_1 was up to 10-fold lower than those developed by $\alpha_4\beta_1$ after background subtraction. The distribution of unbinding (rupture) forces measured for the two integrin variants was, however, similar (Fig. 8 C). Thus, paxillin association with the α_4 subunit dramatically augments the ability of $\alpha_4\beta_1$ to form adhesive tethers that resist disruptive forces irrespective to whether these forces are applied during a vertical force loading (AFM) or during cell rotation (shear stress).

Paxillin association with α_4 augments shear resistance of integrin tethers independent of ligand-induced conformational changes

The aforementioned data suggest that paxillin binding to α_4 is required for mechanical stabilization of cell attachments rather than for cytoplasmic induction of high affinity integrin conformations. Ligand binding to integrins can induce conformational changes in the integrin, resulting in high affinity conformations (Du et al., 1991; Shimaoka et al., 2002). Therefore, we considered the possibility that the reduced tether formation by the α_4(Y991A) mutant could reflect defective, instantaneous ligand-induced conformational changes in the integrin under shear stress. We first verified that the $\alpha_4\beta_1$ ligand Bio1211 provoked similar conformational changes in $\alpha_4\beta_1$ and α_4(Y991A)β_1 under shear-free conditions, as indicated by the identical induction of the β_1 ligand–induced binding site reporter 15/7 epitope by increasing doses of the monovalent $\alpha_4\beta_1$-specific ligand Bio1211 (Fig. 9 A; Lin et al., 1999). We next tested the intrinsic attachment efficacy of either wt α_4 or the α_4Y991A mutant to surface-immobilized α_4 mAb in the absence of ligand occupancy of the integrin. Notably, the HP1/2 mAb binding to α_4 integrins is not sensitive to their affin-

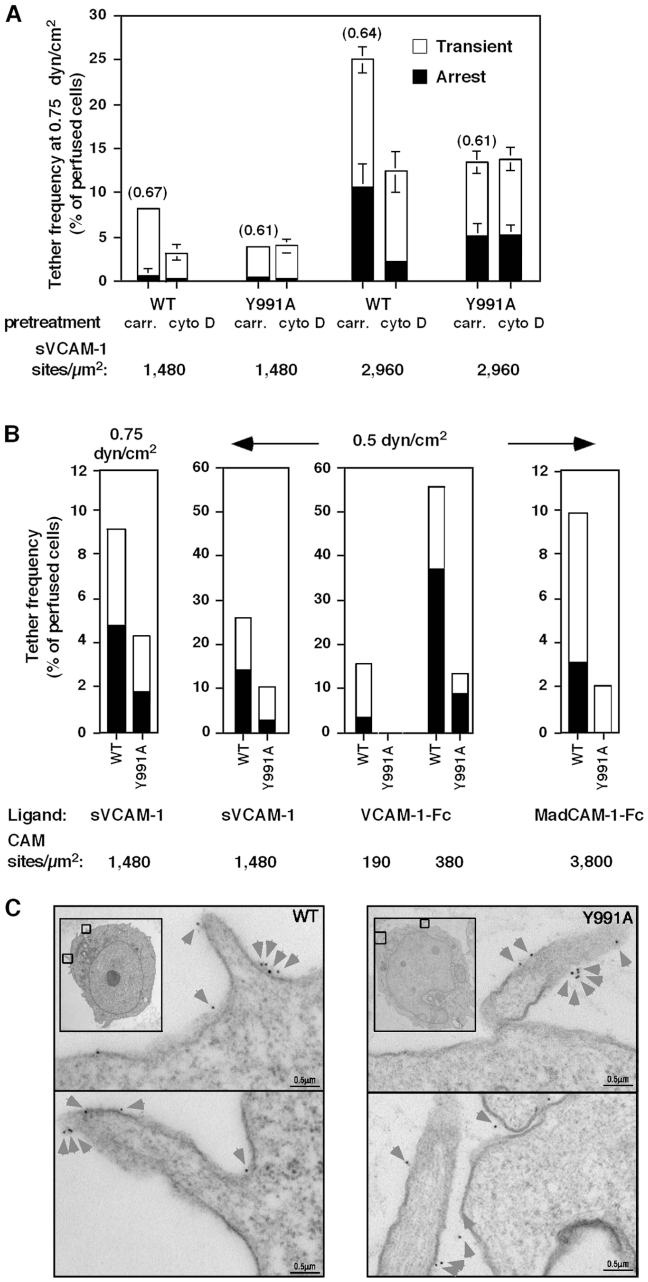

Figure 7. **Paxillin association with the α_4-cytoplasmic tail facilitates tethering mediated by $\alpha_4\beta_1$ and $\alpha_4\beta_7$ under shear flow without altering α_4 distribution on microvilli.** (A) Tethering (transient or followed by immediate arrest) of Jurkat cells expressing either wt α_4 (WT) or the α_4(Y991A) mutant (Y991A) to immobilized VCAM-1. The mean duration of transient tethers is shown in parenthesis above bars. Where indicated, cells were pretreated with 20 μM cytochalasin D (cyto D) or carrier (carr). Error bars represent SD. (B) Tethering under shear flow of Jurkat cells mediated by either WT or Y991A to distinct α_4-integrin ligands. Tethers (transient or arrest) were determined under the indicated shear stresses on surfaces coated with either monomeric 7D VCAM-1 (sVCAM-1), dimeric 7D VCAM-1 (VCAM-1–Fc), or high density MadCAM-Fc. In each panel, the mean ± range of two experimental fields is depicted. All tethers to VCAM-1 were blocked in the presence of the α_4-integrin mAb HP1/2 (not depicted). All tethers to MadCAM-1 were blocked by the anti-$\alpha_4\beta_7$ antibody Act-I (not depicted). Results in A and B are representative of five and four independent experiments, respectively. (C) Surface distribution of wt α_4 (WT) or the α_4(Y991A) mutant on JB4 Jurkat cells monitored by immunoelectron microscopy. Insets show lower magnification images. The boxed areas depict the cellular areas enlarged. Prefixed cells were stained with the nonblocking α_4-specific mAb B5G10. Washed cells were stained with rabbit anti–mouse Ig and 5 nm gold particle–conjugated goat anti–rabbit as described in Materials and methods. Gold particles are marked by arrowheads. Photomicrographs are representative of 20–30 cells.

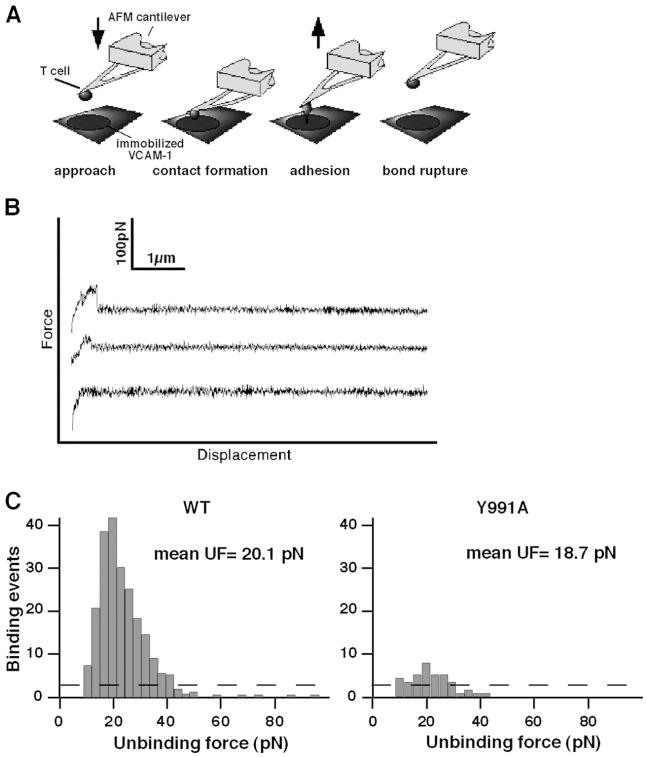

Figure 8. **α_4(Y991A)β_1 fails to stabilize bonds ruptured by an AFM probe.** (A) Schematic representation of the experimental system. JB4 cells were coupled to an AFM cantilever tip via an anti-CD43 mAb. VCAM-Fc was immobilized onto the substrate as in previous figures. (B) Representative AFM force–displacement curves acquired with wt α_4–expressing JB4 cells (top) or α_4(Y991A)-expressing cells (middle) approaching the VCAM-1–Fc-bearing substrate. A force–displacement curve of wt α_4–expressing JB4 approaching a control substrate devoid of VCAM-1 is indicated in the bottom curve. (C) Force histograms of $\alpha_4\beta_1$–VCAM-1 unbinding forces measured under a fixed loading rate of 0.33 nN/s. The number of productive adhesive interactions and their unbinding force distribution are depicted. Background binding is depicted by the dashed line. The mean unbinding force (UF) values of 10 independent experiments are indicated near each histogram. Pulling velocity was 3 μm/s, and the cell–substrate contact time was 0.5 s. A representative result of 10 independent experiments is depicted.

ity to or rearrangement by native ligands (Feigelson et al., 2001) and, thus, should be insensitive to intrinsic or ligand-induced affinity changes under shear stress. Notably, in the presence of shear flow, the α_4(Y991A) mutant formed adhesive tethers to immobilized HP1/2 mAb much less efficiently than wt α_4 (Fig. 9 B), as was observed for VCAM-1 (Fig. 1). In addition, adhesive contacts generated by the α_4(Y991A) mutant after 1 min of static contact also exhibited poor resistance to detachment by increasing shear forces relative to wt α_4–mediated contacts (Fig. 9 C). Thus, paxillin association with the α_4-integrin tail enhances the ability of the integrin subunit to generate resistance to detachment forces independently of ligand-induced conformational rearrangements under shear stress conditions.

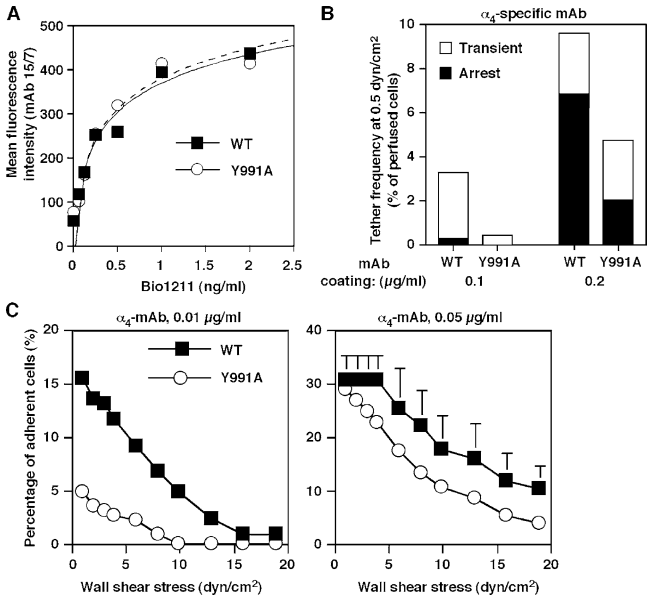

Figure 9. **Paxillin association with α_4 integrins stabilizes adhesive tethers to immobilized α_4-specific mAbs independent of ligand-induced rearrangements.** (A) Dose-dependent induction of the 15/7 epitope by the $\alpha_4\beta_1$-specific ligand Bio1211 on wt α_4 or α_4(Y991A)–expressing Jurkat cells. (B) Reduced tethering and firm adhesion of the α_4(Y991A) mutant to immobilized α_4 mAb (HP1/2) under shear flow. Frequency of tethers and their categories were determined as in Fig. 7. (C) Strength of adhesion developed by JB4 expressing either wt or α_4(Y991A) settled for 1 min on low or high density mAb. Experiments in A and B are each representative of three independent experiments. Error bars represent SD.

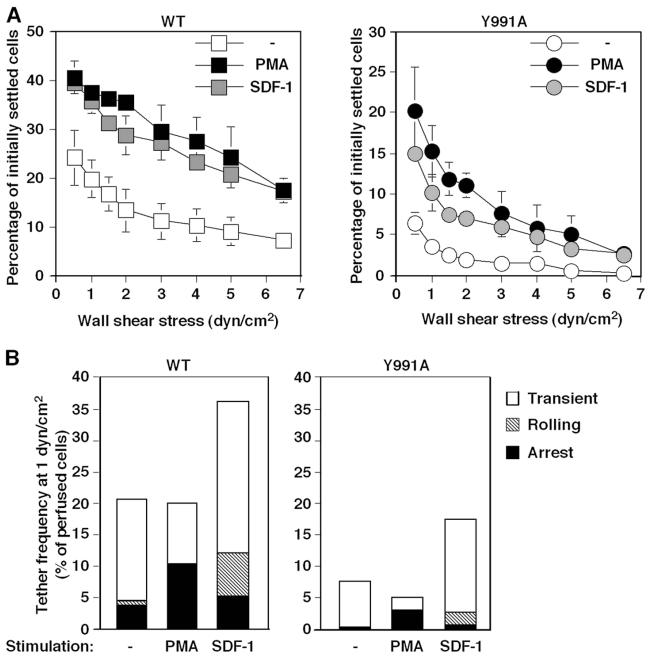

Figure 10. **The α_4(Y991A)β_1 mutant responds to phorbol ester and SDF-1 inside-out signals but develops poor adhesiveness in stimulated T cells under shear flow.** Adhesion of JB4 cells expressing wt α_4 or α_4(Y991A) mutant to sVCAM-1 (2,960 sites/μm^2) left intact (−) or stimulated by 1 min PMA pretreatment or by cell encounter with SDF-1α coimmobilized at 2 μg/ml. (A) Resistance to detachment after 1 min of static contact analyzed as in Fig. 1. Values are mean ± range of two experimental fields. (B) Capture and arrest under continuous shear flow. Frequency of tethers and their categories were determined as in Fig. 7. The experiments in A and B are each representative of four independent tests.

The α_4(Y991A)β_1 mutant responds to inside-out stimulation but develops weaker adhesions to VCAM-1 under shear flow

Cellular stimulation by various agonists increases integrin adhesiveness in various contexts (Hynes, 2002). We next examined the effects of two prototypic agonists, PMA, a direct agonist of diacyl glycerol–dependent PKCs, and the chemokine SDF-1 (CXCL12) on mutant and wt α_4. Exposure of JB4-α_4(Y991A) cells to soluble PMA or to immobilized SDF-1 resulted in enhanced resistance to detachment from VCAM-1–bearing surfaces (Fig. 10 A), although the overall adhesion strength developed by the α_4(Y991A) mutant was lower than that developed by the intact integrin. Further analysis of adhesive tethers formed on VCAM-1 at subsecond contacts also indicated that the ability of initial α_4(Y991A)β_1-dependent Jurkat tethers to convert to immediate firm arrests was enhanced by PMA (Fig. 10 B). Likewise, JB4-α_4(Y991A) cells efficiently responded to in situ subsecond signals from SDF-1 with a twofold elevated frequency of $\alpha_4\beta_1$-dependent tethers on VCAM-1 (Fig. 10 B, right). However, overall SDF-1–stimulated tethers mediated by α_4(Y991A) cells remained lower than wt α_4–mediated tethers. Thus, although the mutant α_4 underwent robust activation in response to both chemokine and PMA inside-out signals, its impaired cytoskeletal associations resulted in overall reduced adhesion to VCAM-1 under shear stress.

Discussion

This study shows that the disruption of paxillin binding to the integrin α_4 tail abrogates its anchorage to the actin cytoskeleton and impairs the ability of integrin ligand bonds to withstand immediate rupture by shear stress, an AFM-pulling device, or abruptly applied magnetic force. Despite normal distribution on the cell surface and retained avidity to immobilized VCAM-1, in the presence of applied forces, this anchorage-deficient mutant poorly mediates tether formation and rapid adhesion strengthening on its ligand. Paxillin-dependent cytoskeletal anchoring of ligand-occupied α_4 integrins may thus underlie their unique capacity to resist disruptive forces and support leukocyte adhesion under shear flow. Thus, although cytoskeletal constraints of integrins were predicted to restrict mobility and clustering on the cell surface and reduce cell adhesiveness (Kucik et al., 1996; Yauch et al., 1997; Kim et al., 2004), we propose that α_4 integrins must retain correct cytoskeletal associations to resist immediate rupture by shear stresses exerted at leukocyte contacts with target blood vessels. Our findings indicate that α_4-integrin anchorage to the cell cytoskeleton is critical for nascent adhesive contacts to resist immediate rupture by shear stress, but it is not required for integrin binding to the ligand nor for ligand-induced conformational rearrangements in the absence of external force. The anchorage deficiency of the α_4-tail mutant resulted in an inability to develop

adhesion to a high affinity mAb, which binds the integrin independently of affinity to native ligands (Feigelson et al., 2001; Kinashi et al., 2004). Altogether, these data suggest that paxillin associations with the α_4 tail control (a postligand occupancy anchorage step that is critical for tether stabilization under stress), which is a mechanical property underlying the ability of lymphocytes to capture and arrest on endothelial α_4-integrin ligands under shear flow. Our experiments on cytokine-activated endothelial cells also predict an increased contribution of this α_4–paxillin association to T cells interacting with endothelial beds expressing α_4-integrin ligands in the absence of endothelial selectins.

Integrin affinity is controlled by β-subunit associations with the talin head domain (Tadokoro et al., 2003) and by Rap1 (Kinashi, 2005) via effectors such as RAPL (regulator of adhesion and cell polarization enriched in lymphoid tissues; Katagiri et al., 2004). The effect of RAPL requires α-tail sequences (Katagiri et al., 2004) that are distant from the paxillin-binding site on α_4 (Liu and Ginsberg, 2000). The retained affinity of the α_4(Y991A) mutant and its capacity to mediate static adhesion suggest that lack of paxillin association with the α_4-integrin tail does not interfere with Rap1-dependent signals whether mediated through RAPL or other Rap1 effectors. The reduction in talin association with α_4(Y991A)β_1 did not alter basal $\alpha_4\beta_1$ affinity for VCAM-1 (Rose et al., 2003), suggesting that the paxillin-mediated association of talin with $\alpha_4\beta_1$ does not contribute to affinity modulation. On the other hand, the extent of these cytoskeletal associations and an intact actin cytoskeleton critically determine the mechanical strength of $\alpha_4\beta_1$ VCAM-1 bonds (i.e., tether formation, adhesion strengthening, and resistance to mechanical stress). Thus, we propose that the ability of α_4 integrins to translate ligand occupancy into immediate mechanical stability of subsecond adhesive contacts requires paxillin and talin-mediated linkages of $\alpha_4\beta_1$ to the actin cytoskeleton. The regulation of $\alpha_4\beta_1$ adhesiveness by talin has never been addressed, especially not under shear stress conditions. The finding that talin suppression impairs the strengthening of wt $\alpha_4\beta_1$ bonds under strain is reminiscent of results reporting the involvement of talin1 in ligand-driven $\alpha_5\beta_1$-cytoskeletal bonds in fibroblasts (Jiang et al., 2003). Although different integrins may anchor differently to the cytoskeleton in distinct cell types, this involvement of talin in both α_4- and α_5-integrin associations with the actin cytoskeleton is consistent with the notion that talin, apart from its role in integrin affinity regulation (Tadokoro et al., 2003), is a key postligand occupancy adaptor that promotes integrin bond stabilization in distinct mechanical contexts and cellular environments.

Our results highlight the role of the α-integrin subunit rather than the β subunit in postligand binding adhesion strengthening of the $\alpha_4\beta_1$–VCAM-1 bond under mechanical strain. Previous findings suggested that a nearly complete truncation of the α_4-cytoplasmic tail impairs $\alpha_4\beta_1$ adhesion strengthening without altering initial cell capture to VCAM-1 under shear flow (Alon et al., 1995; Kassner et al., 1995). This truncation of the α_4-integrin tail also reduced integrin mobility (Yauch et al., 1997) and may have increased integrin cytoskeletal anchorage via the intact β1 subunit, although this was not experimentally demonstrated. Therefore, in these earlier studies, it was impossible to distinguish between the contributions of α_4 anchorage versus mobility to rapid mechanical stabilization of α_4 integrin–mediated tethers. Our present results provide the first direct evidence for a positive role of α_4 anchorage for the earliest stabilization events of $\alpha_4\beta_1$–VCAM-1 bonds subjected to mechanical strain.

In addition to the α_4 Y991 residue, the phosphorylation level of the α_4 serine 988 has been shown to control the degree of α_4 association with paxillin (Han et al., 2001). A dephosphorylated serine variant mimicked by the phosphodeficient mutant α_4 S988A was reported to bind paxillin at enhanced levels (Nishiya et al., 2005). Interestingly, this phosphodeficient mutant did not properly anchor to the cytoskeleton and supported reduced adhesiveness to VCAM-1 (unpublished data). These findings, together with the paxillin-silencing data of this study, suggest that paxillin binding to the α_4 subunit is required but is insufficient to anchor α_4 to the cytoskeleton. Thus, α_4 phosphorylation, which is postulated to attenuate paxillin binding to the α_4 subunit, is in fact required, at least at a basal level, for proper cytoskeletal α_4 association and productive adhesiveness under shear stress. Overphosphorylation of α_4, which reduces paxillin association, may, on the other hand, attenuate both anchorage and adhesiveness. Studies are ongoing to address both the positive and negative effects of serine phosphorylation on α_4 anchorage and function under strain.

α_4 association with paxillin enhances the activation of the focal adhesion kinases FAK and PYK-2 after $\alpha_4\beta_1$ ligation (Liu et al., 1999; Rose et al., 2003). This association also restricts Rac activation at the leading edge via recruitment of the Arf GTPase-activating protein (Nishiya et al., 2005). Nevertheless, at 1-min contacts with VCAM-1, cells expressing the α_4-tail mutant spread normally on VCAM-1. Suppression of tyrosine phosphorylation or inhibition of PYK-2 activity in Jurkat T cells had no effect on $\alpha_4\beta_1$-mediated adhesion strengthening developed under shear stress (unpublished data). Thus, the ability of paxillin association with $\alpha_4\beta_1$ to enhance integrin anchorage to the cytoskeleton and promote mechanical stability of adhesive tethers at short-lived contacts is distinct from its roles in focal adhesion turnover and Rac deactivation during cell spreading on VCAM-1–containing substrates (Nishiya et al., 2005). Altogether, our findings suggest that modulating mechanical properties of α_4 integrins by the inhibition of specific associations between α_4-cytoplasmic tails and the cytoskeleton may be a selective strategy to fine tune integrin-mediated adhesion under shear stress without altering integrin affinity.

Materials and methods

Reagents and antibodies

Recombinant seven-domain human VCAM-1 (sVCAM-1) was provided by B. Pepinsky (Biogen, Cambridge, MA). VCAM-1–Fc fusion protein containing seven-domain VCAM-1 fused to IgG was generated as described previously (Rose et al., 2000). VCAM-1–Fc constructed from domains 1 and 2 of VCAM-1 fused to Fc, termed 2D VCAM-1–Fc, was provided by B. Pepinsky. Affinity-purified human full-length spleen-derived ICAM-1 was a gift from T. Springer (Harvard University, Boston, MA). ICAM-Fc and SDF-1α were purchased from R&D Systems. BSA (fraction V), poly-L-lysine, and Ca^{2+}/Mg^{2+}-free HBSS were obtained from Sigma-Aldrich. Human serum albumin (fraction V) and PMA were purchased from Calbiochem.

The α_4-integrin function–blocking HP1/2 mAb, the E-selectin–blocking mAb BB11, the β_1-specific TS2/16 mAb, the α_4-specific nonblocking 5BG10 mAb (all provided by B. Pepinsky), the β_1-integrin subunit mAb 15/7 (provided by T. Yednock, Elan Pharmaceuticals, San Francisco, CA; Yednock et al., 1995), and the anti-$\alpha_4\beta_7$ Act-1 (a gift from M.J. Briskin, Millennium Pharmaceuticals, Cambridge, MA) were all used as purified Ig. Antitalin mAb (clone 8d4) was purchased from Sigma-Aldrich. Anti-paxillin mAb (clone 349) was purchased from BD Transduction Laboratories. Goat polyclonal anti-α_4 Ab (clone C-20) was purchased from Santa Cruz Biotechnology, Inc.

Cell culture and flow cytometry

Jurkat cells deficient in α_4 (JB4) were stably transfected with either wt α_4 or α_4(Y991A) cDNA as described previously (Liu et al., 1999). Cells were subcloned, and multiple clones expressing identical levels of α_4 and β_1 subunits were taken for functional analysis. Clones were maintained in RPMI 1640 medium supplemented with 10% heat-inactivated FCS, 2 mM L-glutamine, 1 mM sodium pyruvate, 100 mM nonessential amino acids, and antibiotics (Biological Industries). Primary HUVECs were established as previously described (Shamri et al., 2005). HUVECs were left intact or stimulated for 4 h with 0.1 ng/ml TNF-α (R&D Systems) before experiments. Staining and FACS analysis were performed as previously described (Feigelson et al., 2003).

Immunofluorescence staining and immunoelectron microscopy

For α_4-integrin immunostaining, Jurkat cells were washed in PBS and incubated with 10 μg/ml anti-α_4 B5G10 mAb for 30 min at 4°C. Cells were washed once with PBS + 5 mM EDTA and twice with PBS/0.1% BSA, and α_4 integrins were stained with AlexaFluor546-conjugated anti–mouse Ab (Invitrogen) and fixed in 3% PFA in PBS (30 min at RT). Control cells were fixed before mAb incubation steps. Cells were attached to poly-L-lysine–coated glass slides, and coverslips were mounted with elvanol overnight and analyzed with a confocal microscope (TE300; Nikon) and a laser-scanning system (model 2000; Bio-Rad Laboratories).

α_4 localization was assessed by immunoelectron microscopy as previously described (Chen et al., 1999). In brief, cultured Jurkat cells were washed and prefixed in 0.1 M phosphate buffer, pH 7.4, containing 2% PFA and 0.05% glutaraldehyde. Washed cells in H/H medium (HBSS containing 2 mg/ml BSA and 10 mM Hepes, pH 7.4, supplemented with 1 mM $CaCl_2$ and 1 mM $MgCl_2$) were incubated with 10 μg/ml anti-α_4 B5G10 mAb for 40 min at 22°C. Washed cells were stained with 10 μg/ml rabbit anti–mouse Ig, washed, and incubated for 45 min with 5 nm gold particle–conjugated goat anti–rabbit (Aurion). Ultrathin sections (70–90 nm) of 40–60 cells for each experimental group were examined with an electron microscope (Tecnai 12; FEI) under 120 kV, and images were taken using a CCD camera (Megaview 3; Soft Imaging System). In each experimental group analyzed, the number of α_4-specific gold particles on microvillar projections was compared with that on adjacent cell body compartments of identical dimensions.

siRNA-mediated silencing of paxillin and talin

Silencing of talin expression in Jurkat cells was achieved by a talin1-specific 21-nucleotide siRNA (Dharmacon) corresponding to positions 6,043–6,063 relative to the talin1 mRNA start codon (Shamri et al., 2005). Silencing of paxillin was conducted as described previously (Nishiya et al., 2005). Control transfections were performed with a fluorescein-labeled 21-nucleotide duplex directed to Luciferase GL2. Transfection of T cells was performed by electroporation using the Nucleofection system (Amaxa). Transfected cells were maintained in culture medium. Talin and paxillin expression monitored by immunoblotting was maximally suppressed 72 h posttransfection, and time points were chosen for subsequent functional assays. Immunoprecipitation of α_4 was performed as previously described (Feigelson et al., 2003).

Quantification of integrin anchorage to the cytoskeleton

Cells were stained with 10 μg/ml of the FITC-conjugated anti-α_4 mAb HP1/2 at 4°C for 30 min, washed twice with H/H medium supplemented with 1 mM $CaCl_2$ and 1 mM $MgCl_2$, and left either untreated or cross-linked with secondary antibodies at 4°C for 30 min followed by two washes as described previously (Geppert and Lipsky, 1991; Evans et al., 1999). All cells were then incubated at RT for 30 min with the cytoskeletal stabilizing buffer (CSB; 50 mM NaCl, 2 mM $MgCl_2$, 0.22 mM EGTA, 13 mM Tris, pH 8.0, 1 mM PMSF, 10 mM iodacetamide, and 2% FCS) alone or supplemented with 0.1% NP-40. The intact cells or their recovered detergent-insoluble cytoskeletal fractions were washed in detergent-free CSB, fixed in 1% PFA/PBS, and analyzed by flow cytometry. Under these conditions, the majority of detergent-treated cells retain their shape and size. The ratio of mean fluorescence intensity recovered in detergent-treated cells divided by that of cells not exposed to the detergent yields the fraction of mAb-bound α_4 integrin that is resistant to detergent extraction; i.e., anchored to the (detergent resistant) cytoskeletal fraction of the cell.

VCAM-1 microbead–binding assays and integrin bond stiffness

Protein A–coated magnetic M-280 Dynabeads (Dynal) were coated at RT with various concentrations (0.004–1 μg/ml) of 2D VCAM-Fc in H/H binding medium, washed according to the manufacturer's instructions, and stored on ice. Cells and VCAM-1–coated beads were mixed at RT for 1 min in binding medium at a concentration of 10^7 cells/ml at a cell/bead ratio of 1:8 followed by a threefold dilution in binding medium. The cellular side scatter, distinguishing between bead-bound and bead-free cells, was analyzed immediately in a FACScan flow cytometer (Becton Dickinson). Background binding determined with protein A–coated beads was <10% of the maximal binding observed at VCAM-1 saturation and was subtracted from the total binding results.

The mechanical stiffness of $\alpha_4\beta_1$/VCAM-1 adhesions was measured by electromagnetic pulling cytometry using VCAM-1–coated beads (Matthews et al., 2004). The detailed method is described in supplemental material (available at http://www.jcb.org/cgi/content/full/jcb.200503155/DC1).

AFM measurements

All force measurements were conducted at 35 ± 2°C using a previously described AFM apparatus (Benoit et al., 2000). In brief, a microfabricated Si_3N_4 cantilever tip (Park Scientific Instruments) was coated with 0.1 mg/ml of the anti-CD43 mAb (R&D Systems). The spring constants of the cantilevers used were determined at ~4.7 ± 0.6 mN/m. A single cell was immobilized on the cantilever tip shortly before experimentation. The device was mounted with a piezo-actuator (Piezosystem Jena) on an inverted optical microscope (Carl Zeiss MicroImaging, Inc.) containing a heating stage. A diode laser beam focused on the sensor was used to measure the displacement of the cantilever by the laser beam deflection on a two-segment photodetector. The cell adhering to the cantilever was positioned above an adhesive substrate coated with 2D VCAM-1–Fc captured via human IgG Fc mAb (Jackson ImmunoResearch Laboratories). The cantilever was lowered until the sensor detected a contact force equal to a preselected value (typically 50 pN). After the contact was established for a dwelling time of 500 ms, the cell-bearing cantilever was lifted up by the piezo-actuator, and the de-adhesion force was monitored by a force–distance plot (Fig. 5 B). From this plot, the last detectable de-adhesion force was calculated. For each cell, ~50–200 force–distance plots were collected within ~30 min. All de-adhesion events collected in at least 10 independent experiments were presented in histograms (Fig. 5 C).

Laminar flow adhesion assays

Purified ligands or mAbs were coated on polystyrene plates as previously described (Grabovsky et al., 2000). Site densities of coated sVCAM-1 and VCAM-1–Fc were determined as previously described (Grabovsky et al., 2000; Sigal et al., 2000). The polystyrene plates were each assembled on the lower wall of the flow chamber (260-um gap) as previously described (Dwir et al., 2000; Feigelson et al., 2001). Cells were washed with cation-free H/H medium, resuspended in binding medium (H/H medium supplemented with 1 mM $CaCl_2$ and 1 mM $MgCl_2$), and perfused through the flow chamber at the desired shear stress. To disrupt actin cytoskeleton, cells were pretreated for 15 min with 20 μM cytochalasin D (Calbiochem) or carrier solution (0.1% DMSO). All flow experiments were conducted at 37°C. Tethers were defined as transient if cells attached briefly (<2 s) to the substrate and as arrests if they immediately arrested and remained stationary for at least 5 s of continuous flow. Frequencies of adhesive categories within differently pretreated cells or rates of cell accumulation on adhesive substrates were determined as a percentage of cells flowing immediately over the substrates, as previously described (Grabovsky et al., 2000). To assess rapid development of integrin avidity to the ligand at 1-min stationary contacts, cells were allowed to settle onto the substrate for 1 min at stasis. Flow was then initiated and increased step-wise every 5 s by a programmed set of rates. At the indicated shear stresses, the number of cells that remained bound was expressed relative to the number of cells originally settled on the substrate. Over 95% of tethers to VCAM-1 were blocked by pretreating cells with 10 μg/ml of the α_4-blocking mAb HP1/2. Live imaging of α_4 on Jurkat cells prelabeled with AlexaFluor488-conjugated B5G10 mAb that settled on VCAM-1 was conducted with Delta Vision Spectris RT (Applied Precision). α_4 patching was quantified using Image J software (National Institutes of Health).

Online supplemental material

Fig. S1 shows the analysis of VCAM-1–coated bead displacement during a magnetic force pulse applied on wt Jurkat cells. The supplemental Materials and methods section describes the experimental setup.

We thank S. Schwarzbaum for editorial assistance.

R. Alon is the Incumbent of The Tauro Career Development Chair in Biomedical Research. This research was supported by the Fogarty International Research Collaboration Awards and was partially supported by the Israel Science Foundation and MAIN, the EU6 Program for Migration and Inflammation. This work was also supported by National Institutes of Health (NIH) grants AR27214 and HL57009 to M.H. Ginsberg, NIH grant CA45548 to D.E. Ingber, and NIH grant P30AR47360 to D.M. Rose. The work of D.M. Rose was additionally supported by the Department of Veterans Affairs Merit Review Entry Program Award and by the Arthritis Foundation.

Submitted: 28 March 2005
Accepted: 8 November 2005

References

Alon, R., and S. Feigelson. 2002. From rolling to arrest on blood vessels: leukocyte tap dancing on endothelial integrin ligands and chemokines at subsecond contacts. *Semin. Immunol.* 14:93–104.

Alon, R., P.D. Kassner, M.W. Carr, E.B. Finger, M.E. Hemler, and T.A. Springer. 1995. The integrin VLA-4 supports tethering and rolling in flow on VCAM-1. *J. Cell Biol.* 128:1243–1253.

Ambroise, Y., B. Yaspan, M.H. Ginsberg, and D.L. Boger. 2002. Inhibitors of cell migration that inhibit intracellular paxillin/alpha4 binding: a well-documented use of positional scanning libraries. *Chem. Biol.* 9:1219–1226.

Benoit, M., D. Gabriel, G. Gerisch, and H.E. Gaub. 2000. Discrete interactions in cell adhesion measured by single-molecule force spectroscopy. *Nat. Cell Biol.* 2:313–317.

Berlin, C., E.L. Berg, M.J. Briskin, D.P. Andrew, P.J. Kilshaw, B. Holzmann, I.L. Weissman, A. Hamann, and E.C. Butcher. 1993. $\alpha_4\beta_7$ integrin mediates lymphocyte binding to the mucosal vascular addressin MAdCAM-1. *Cell.* 74:185–195.

Berlin, C., R.F. Bargatze, J.J. Campbell, U.H. von Andrian, M.C. Szabo, S.R. Hasslen, R.D. Nelson, E.L. Berg, S.L. Erlandsen, and E.C. Butcher. 1995. α_4 integrins mediate lymphocyte attachment and rolling under physiologic flow. *Cell.* 80:413–422.

Brown, M.C., and C.E. Turner. 2004. Paxillin: adapting to change. *Physiol. Rev.* 84:1315–1339.

Carman, C.V., and T.A. Springer. 2003. Integrin avidity regulation: are changes in affinity and conformation underemphasized? *Curr. Opin. Cell Biol.* 15:547–556.

Chen, C., J.L. Mobley, O. Dwir, F. Shimron, V. Grabovsky, R.L. Lobb, Y. Shimizu, and R. Alon. 1999. High affinity VLA-4 subsets expressed on T cells are mandatory for spontaneous adhesion strengthening but not for rolling on VCAM-1 in shear flow. *J. Immunol.* 162:1084–1095.

Constantin, G., M. Majeed, C. Giagulli, L. Piccio, J.Y. Kim, E.C. Butcher, and C. Laudanna. 2000. Chemokines trigger immediate β_2 integrin affinity and mobility changes: differential regulation and roles in lymphocyte arrest under flow. *Immunity.* 13:759–769.

Du, X.P., E.F. Plow, A.L. Frelinger 3rd, T.E. O'Toole, J.C. Loftus, and M.H. Ginsberg. 1991. Ligands "activate" integrin alpha IIb beta 3 (platelet GPIIb-IIIa). *Cell.* 65:409–416.

Dwir, O., G.S. Kansas, and R. Alon. 2000. An activated L-selectin mutant with conserved equilibrium binding properties but enhanced ligand recognition under shear flow. *J. Biol. Chem.* 275:18682–18691.

Dwir, O., G.S. Kansas, and R. Alon. 2001. The cytoplasmic tail of L-selectin regulates leukocyte capture and rolling by controlling the mechanical stability of selectin:ligand tethers. *J. Cell Biol.* 155:145–156.

Evans, S.S., D.M. Schleider, L.A. Bowman, M.L. Francis, G.S. Kansas, and J.D. Black. 1999. Dynamic association of L-selectin with the lymphocyte cytoskeletal matrix. *J. Immunol.* 162:3615–3624.

Feigelson, S.W., V. Grabovsky, E. Winter, L.L. Chen, R.B. Pepinsky, T. Yednock, D. Yablonski, R. Lobb, and R. Alon. 2001. The src kinase p56Lck upregulates VLA-4 integrin affinity: implications for rapid spontaneous and chemokine-triggered T cell adhesion to VCAM-1 and fibronectin. *J. Biol. Chem.* 276:13891–13901.

Feigelson, S.W., V. Grabovsky, R. Shamri, S. Levy, and R. Alon. 2003. The CD81 tetraspanin facilitates instantaneous leukocyte VLA-4 adhesion strengthening to VCAM-1 under shear flow. *J. Biol. Chem.* 278:51203–51212.

Firrell, J.C., and H.H. Lipowsky. 1989. Leukocyte margination and deformation in mesenteric venules of rat. *Am. J. Physiol.* 256:H1667–H1674.

Geppert, T.D., and P.E. Lipsky. 1991. Association of various T cell-surface molecules with the cytoskeleton. Effect of cross-linking and activation. *J. Immunol.* 146:3298–3305.

Grabovsky, V., S. Feigelson, C. Chen, R. Bleijs, A. Peled, G. Cinamon, F. Baleux, F. Arenzana-Seisdedos, T. Lapidot, Y. van Kooyk, et al. 2000. Subsecond induction of α_4 integrin clustering by immobilized chemokines enhances leukocyte capture and rolling under flow prior to firm adhesion to endothelium. *J. Exp. Med.* 192:495–505.

Han, J., S. Liu, D.M. Rose, D.D. Schlaepfer, H. McDonald, and M.H. Ginsberg. 2001. Phosphorylation of the integrin alpha 4 cytoplasmic domain regulates paxillin binding. *J. Biol. Chem.* 276:40903–40909.

Hynes, R.O. 2002. Integrins: bidirectional, allosteric signaling machines. *Cell.* 110:673–687.

Jiang, G., G. Giannone, D.R. Critchley, E. Fukumoto, and M.P. Sheetz. 2003. Two-piconewton slip bond between fibronectin and the cytoskeleton depends on talin. *Nature.* 424:334–337.

Kansas, G.S., K. Ley, J.M. Munro, and T.F. Tedder. 1993. Regulation of leukocyte rolling and adhesion to high endothelial venules through the cytoplasmic domain of L-selectin. *J. Exp. Med.* 177:833–838.

Kassner, P.D., R. Alon, T.A. Springer, and M.E. Hemler. 1995. Specialized functional properties of the integrin α_4 cytoplasmic domain. *Mol. Biol. Cell.* 6:661–674.

Katagiri, K., N. Ohnishi, K. Kabashima, T. Iyoda, N. Takeda, Y. Shinkai, K. Inaba, and T. Kinashi. 2004. Crucial functions of the Rap1 effector molecule RAPL in lymphocyte and dendritic cell trafficking. *Nat. Immunol.* 5:1045–1051.

Kim, M., C.V. Carman, W. Yang, A. Salas, and T.A. Springer. 2004. The primacy of affinity over clustering in regulation of adhesiveness of the integrin $\alpha_L\beta_2$. *J. Cell Biol.* 167:1241–1253.

Kinashi, T. 2005. Intracellular signalling controlling integrin activation in lymphocytes. *Nat Rev Immunol*. 5:546–559.

Kinashi, T., M. Aker, M. Sokolovsky-Eisenberg, V. Grabovsky, C. Tanaka, R. Shamri, S. Feigelson, A. Etzioni, and R. Alon. 2004. LAD-III, a leukocyte adhesion deficiency syndrome associated with defective Rap1 activation and impaired stabilization of integrin bonds. *Blood.* 103:1033–1036.

Kucik, D.F., M.L. Dustin, J.M. Miller, and E.J. Brown. 1996. Adhesion-activating phorbol ester increases the mobility of leukocyte integrin LFA-1 in cultured lymphocytes. *J. Clin. Invest.* 97:2139–2144.

Lin, K., H.S. Ateeq, S.H. Hsiung, L.T. Chong, C.N. Zimmerman, A. Castro, W.C. Lee, C.E. Hammond, S. Kalkunte, L.L. Chen, et al. 1999. Selective, tight-binding inhibitors of integrin $\alpha_4\beta_1$ that inhibit allergic airway responses. *J. Med. Chem.* 42:920–934.

Liu, S., and M.H. Ginsberg. 2000. Paxillin binding to a conserved sequence motif in the α_4 integrin cytoplasmic domain. *J. Biol. Chem.* 275:22736–22742.

Liu, S., S.M. Thomas, D.G. Woodside, D.M. Rose, W.B. Kiosses, M. Pfaff, and M.H. Ginsberg. 1999. Binding of paxillin to α_4 integrins modifies integrin-dependent biological responses. *Nature.* 402:676–681.

Matthews, B.D., D.R. Overby, F.J. Alenghat, J. Karavitis, Y. Numaguchi, P.G. Allen, and D.E. Ingber. 2004. Mechanical properties of individual focal adhesions probed with a magnetic microneedle. *Biochem. Biophys. Res. Commun.* 313:758–764.

Nishiya, N., W.B. Kiosses, J. Han, and M.H. Ginsberg. 2005. An α_4 integrin-paxillin-Arf-GAP complex restricts Rac activation to the leading edge of migrating cells. *Nat. Cell Biol.* 7:343–352.

Rose, D.M., P.M. Cardarelli, R.R. Cobb, and M.H. Ginsberg. 2000. Soluble VCAM-1 binding to α_4 integrins is cell-type specific and activation dependent and is disrupted during apoptosis in T cells. *Blood.* 95:602–609.

Rose, D.M., S. Liu, D.G. Woodside, J. Han, D.D. Schlaepfer, and M.H. Ginsberg. 2003. Paxillin binding to the α_4 integrin subunit stimulates LFA-1 (integrin $\alpha_L\beta_2$)-dependent T cell migration by augmenting the activation of focal adhesion kinase/proline-rich tyrosine kinase-2. *J. Immunol.* 170:5912–5918.

Shamri, R., V. Grabovsky, J.M. Gauguet, S. Feigelson, E. Manevich, W. Kolanus, M.K. Robinson, D.E. Staunton, U.H. von Andrian, and R. Alon. 2005. Lymphocyte arrest requires instantaneous induction of an extended LFA-1 conformation mediated by endothelium-bound chemokines. *Nat. Immunol.* 6:497–506.

Shimaoka, M., J. Takagi, and T.A. Springer. 2002. Conformational regulation of integrin structure and function. *Annu. Rev. Biophys. Biomol. Struct.* 31:485–516.

Sigal, A., D.A. Bleijs, V. Grabovsky, S.J. van Vliet, O. Dwir, C.G. Figdor, Y. van Kooyk, and R. Alon. 2000. The LFA-1 integrin supports rolling adhesions on ICAM-1 under physiological shear flow in a permissive cellular environment. *J. Immunol.* 165:442–452.

Springer, T.A. 1994. Traffic signals for lymphocyte recirculation and leukocyte emigration: the multistep paradigm. *Cell.* 76:301–314.

Tadokoro, S., S.J. Shattil, K. Eto, V. Tai, R.C. Liddington, J.M. de Pereda, M.H.

Ginsberg, and D.A. Calderwood. 2003. Talin binding to integrin beta tails: a final common step in integrin activation. *Science.* 302:103–106.

van Kooyk, Y., and C.G. Figdor. 2000. Avidity regulation of integrins: the driving force in leukocyte adhesion. *Curr. Opin. Cell Biol.* 12:542–547.

von Andrian, U.H., S.R. Hasslen, R.D. Nelson, S.L. Erlandsen, and E.C. Butcher. 1995. A central role for microvillous receptor presentation in leukocyte adhesion under flow. *Cell.* 82:989–999.

Yauch, R.L., D.P. Felsenfeld, S.K. Kraeft, L.B. Chen, M.P. Sheetz, and M.E. Hemler. 1997. Mutational evidence for control of cell adhesion through integrin recruitment, independent of ligand binding. *J. Exp. Med.* 186: 1347–1355.

Yednock, T.A., C. Cannon, C. Vandevert, E.G. Goldbach, G. Shaw, D.K. Ellis, C. Liaw, L.C. Fritz, and L.I. Tanner. 1995. $\alpha_4\beta_1$ integrin-dependent cell adhesion is regulated by a low affinity receptor pool that is conformationally responsive to ligand. *J. Biol. Chem.* 270:28740–28750.

Zhang, X., S.E. Craig, H. Kirby, M.J. Humphries, and V.T. Moy. 2004. Molecular basis for the dynamic strength of the integrin $\alpha_4\beta_1$/VCAM-1 interaction. *Biophys. J.* 87:3470–3478.